CHAPTER IV
RESULTS AND DISCUSSION

4.1 Response Time of pH Electrode

The method for determining the response time constant (α_e) of the pH electrode is described in Appendix A (Figure A1). The value of this constant needs to be determined because the pH electrode cannot instantaneously measure the pH value of the solution. The response time constant (α_e) can be found from equation (2.9).

$$\frac{dh_m}{dt} = \alpha_e(h_0 - h_m) \tag{2.9}$$

By fitting the experimental data with the equation using the Solver tool in Excel, α_e can be determined as shown in Tables 4.1 and 4.2 for batch and continuous operation, respectively. The plots of predicted and experimental hydrogen ion concentrations versus time are shown in Appendix A.

Table 4.1 Summary of response time constants of pH electrode for batch operation

Mixing Speed (rpm)	Response time constant (sec^{-1})			Response time (sec)
	Run 1	Run 2	Avg.	
250	0.02069	0.01799	0.01934	120
500	0.02286	0.02303	0.02294	101
750	0.02698	0.02680	0.02689	86
1000	0.02484	0.02598	0.02541	91

Table 4.1 shows the response time constant at various mixing speeds (250, 500, 750, 1000 rpm) for the batch operation. The relationship between mixing speed and response time shows that the response time is inversely proportional with the

mixing speed. In other words, a high mixing speed results in faster detection of the pH value of the solution. The results can be explained by the effect of mixing speed on the thickness of the stagnant liquid film, which exists near the surface of the pH electrode. The higher the mixing speed (higher shear force), the lower the thickness of the film, which increases the diffusion of the H^+ ions into the inner core of the pH probe. Furthermore, the last two values of the response time change very little when the mixing speed is changed from 750 to 1000 rpm. It means that at mixing speeds of 750 rpm or higher the film diffusion step is overcome.

Table 4.2 Summary of response time constants of pH electrode for continuous operation

Flow Rate (ml/min)	Response time constant (sec^{-1})			Response time (sec)
	Run 1	Run 2	Avg.	
100	0.00939	0.00999	0.00969	238
150	0.01171	0.01038	0.01105	209
170	0.01334	0.01320	0.01327	174
200	0.02109	0.02020	0.02064	113
220	0.02298	0.02298	0.02298	101
250	0.02272	0.02272	0.02272	102

Table 4.2 shows the response time constants at various flow rates of 0.2 N HCl (100, 150, 170, 200, 220, and 250 rpm) for continuous operation. Similar to the batch operation, the relationship between flow rate of 0.2 N HCl and response time reveals that the response time is inversely proportional with the flow rate. The results can be explained by the same reason as in the case of batch operation. In addition, the flow rate in continuous operation above 220 ml/min makes the effects of both film diffusion and the distance that the solution travels to meet the pH probe vanished.

From the results of both batch and continuous operations, the response time of the pH electrode was found to be in a range of 90-240 seconds (see calculations in Appendix A), which is too high. From these results, it is impossible to measure

adsorption rate that occurs very fast (roughly within 10-20 seconds) with a pH electrode that takes 90-240 seconds to response. So, the new technique of operation was used where the pH value of each sample was measured at equilibrium (see sections 3.3.2 and 3.3.4).

4.2 Batch Operation

For the batch operation, adsorption experiments were carried out in order to develop:

1. Adsorption isotherm which is a relationship between the concentrations of metal ions on the resin and in the solution at equilibrium (q^e and c^e).
2. An expression for the rate of adsorption.

4.2.1 Adsorption Isotherms

The objective in this phase of study is to find the relationship between metal ion concentrations on the resin and in the solution at equilibrium (q^e and c^e) for both in single-ion and mixed-ion systems.

The initial concentration of $CaCl_2$, $MgCl_2$ or $CaCl_2/MgCl_2$ was varied from 0.05 to 0.5 N and the metal concentrations in the resin phase (q^e) were plotted with the corresponding equilibrium concentrations (c^e) as shown in Figure 4.1 to 4.4. The relationship used in this study is Freundlich isotherm, which is shown in equation (4.1).

$$q^e = \beta(c^e)^{1/n} \tag{4.1}$$

where β and n are constant and determined experimentally.

From several sets of the experiments (Figure 4.1 to 4.4), the β and n values for single-ion system of Ca^{2+}, single-ion system of Mg^{2+} and mixed-ion system of Ca^{2+}/ Mg^{2+} can be determined by fitting experimental data with equation (4.1). The β and n values are shown in Table 4.3.

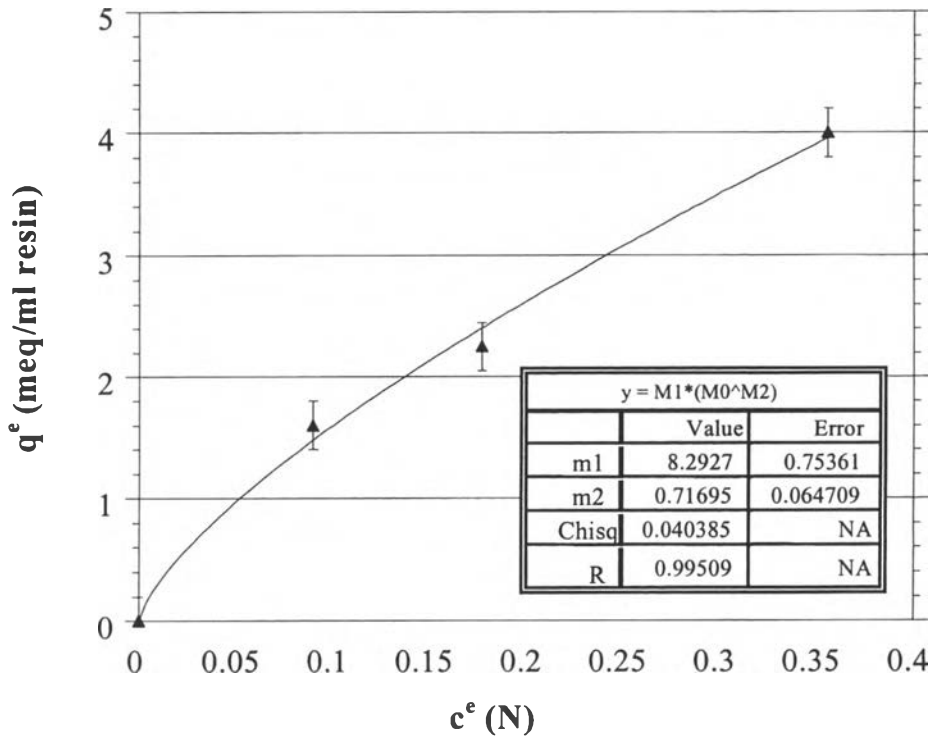

Figure 4.1 Adsorption isotherm of calcium on Dowex50-x8 in single-ion system

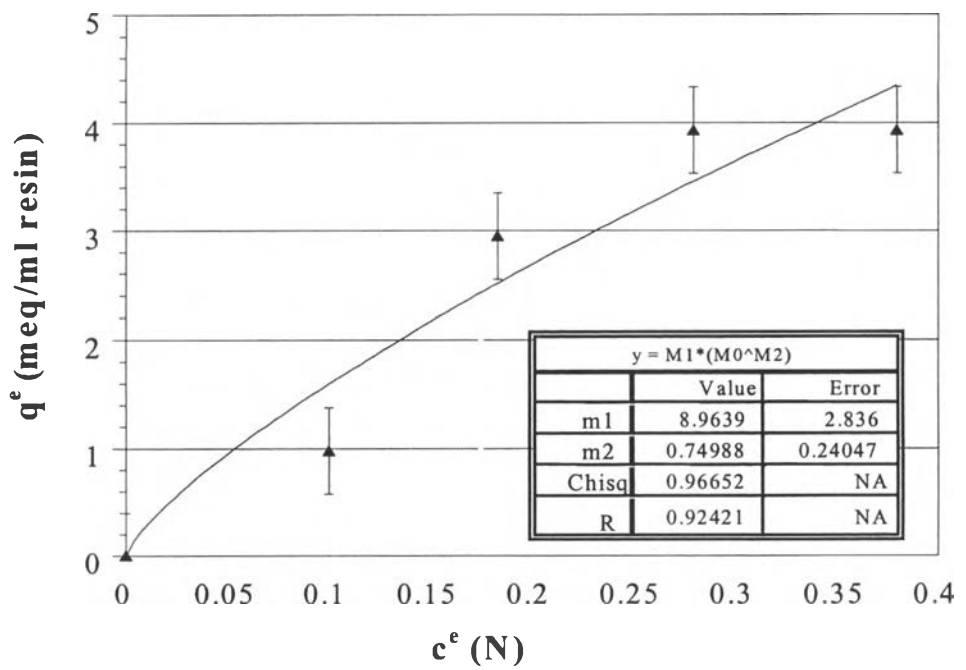

Figure 4.2 Adsorption isotherm of magnesium on Dowex50-x8 in single-ion system

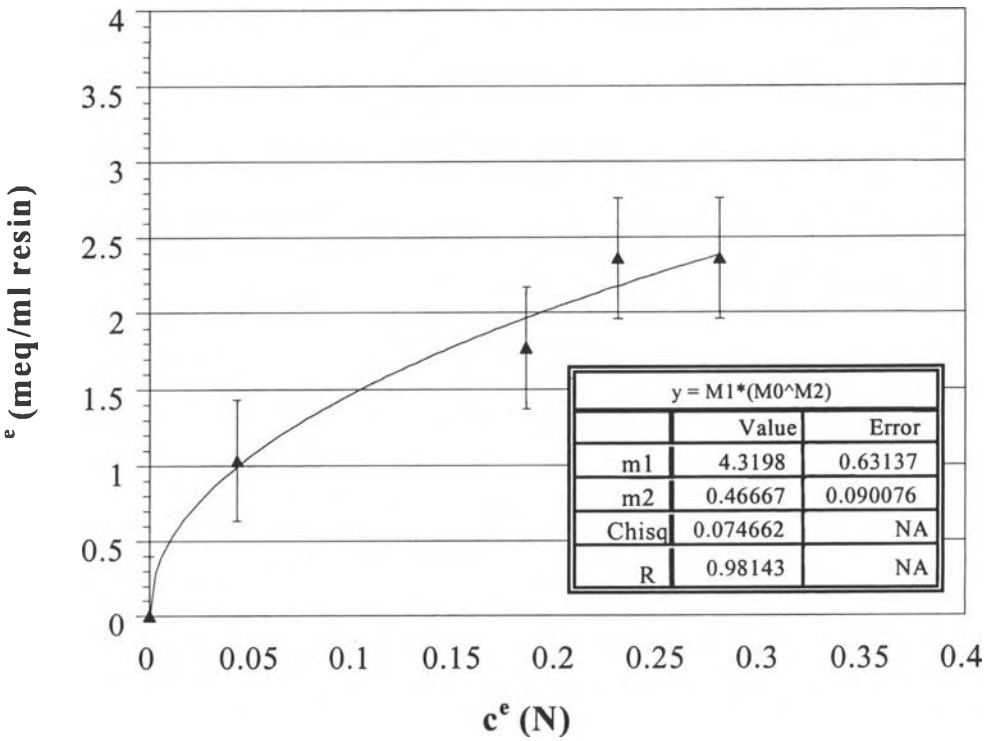

Figure 4.3 Adsorption isotherm of calcium on Dowex50-x8 in mixed-ion system

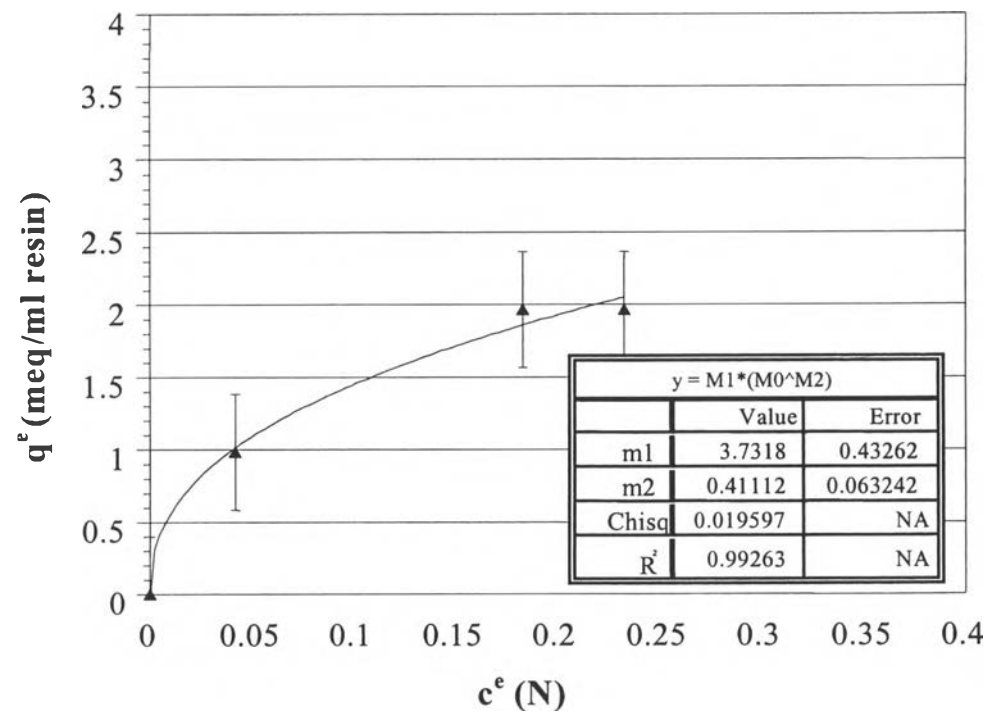

Figure 4.4 Adsorption isotherm of magnesium on Dowex50-x8 in mixed-ion system

Table 4.3 Summary of β and n value in various types of systems

Type of system	β	n
Ca^{2+} in single-ion solution	8.29	1.39
Mg^{2+} in single-ion solution	8.96	1.33
Ca^{2+} in mixed-ion solution	4.32	2.14
Mg^{2+} in mixed-ion solution	3.73	2.43

4.2.2 Rate of Adsorption

The single-ion and mixed-ion adsorption of Ca^{2+} and Mg^{2+} onto the Dowex50-x8 resin at two different initial concentrations (0.2 and 0.6 N) as a function of time are shown in Figure 4.5 and 4.6, respectively.

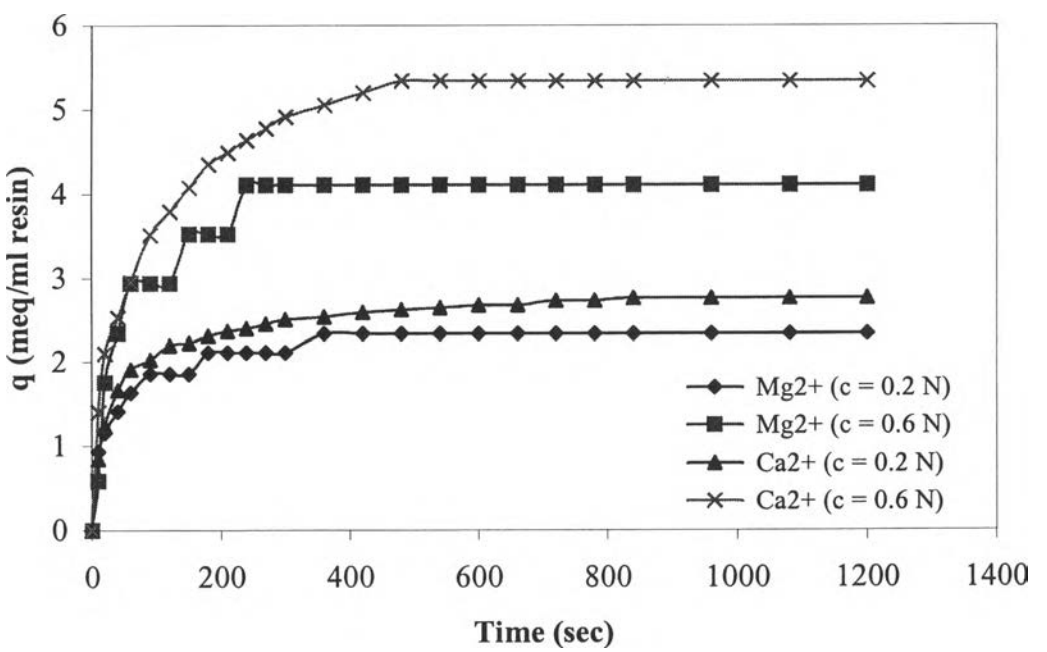

Figure 4.5 Single-ion adsorption of Ca^{2+} and Mg^{2+} onto the resin at two different initial concentrations as a function of time for the batch operation

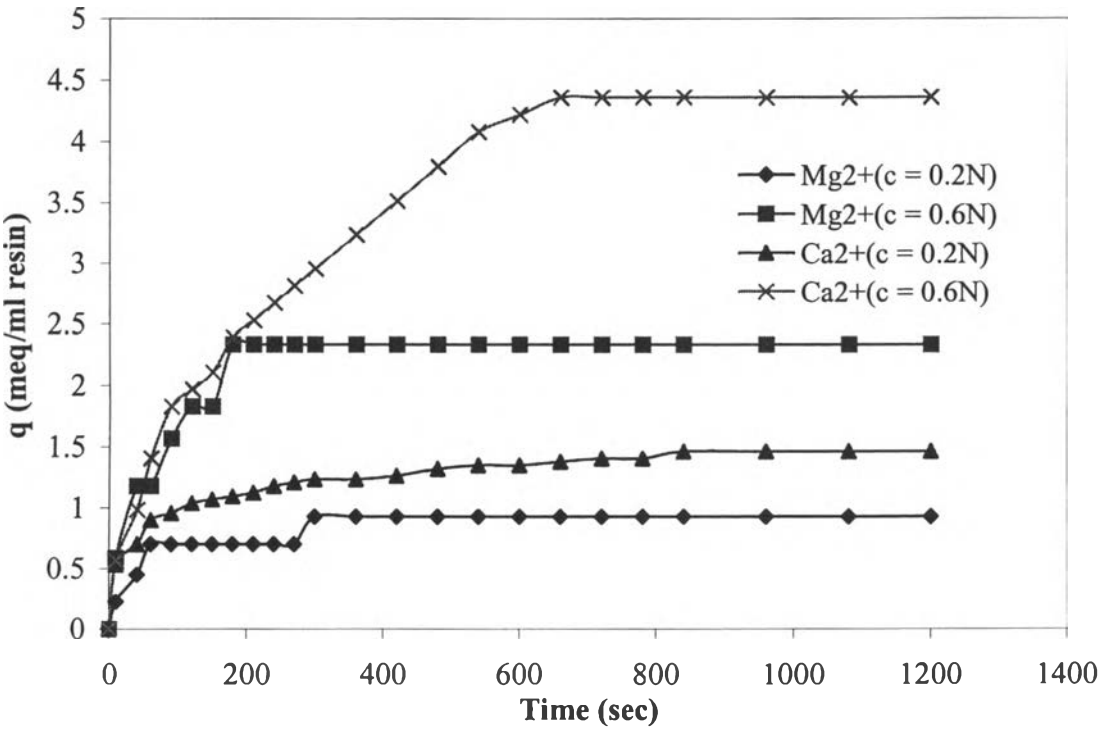

Figure 4.6 Mixed-ion adsorption of Ca^{2+} and Mg^{2+} onto the resin at two different initial concentrations as a function of time for the batch operation

From the shape of the curves in both single-ion and mixed-ion systems, the adsorption of metal ions as represented by q increases very fast at the beginning due to the high concentration gradient. As the adsorption proceeds, the change in q is smaller and the value becomes constant when reaching equilibrium. At the equilibrium, the rate of adsorption, dq/dt as shown in equation (4.2), must be equal to zero.

$$r = \frac{dq}{dt} = K\left(q^e - q\right) \tag{4.2}$$

The rate constant, K, in the adsorption rate equation can be determined from the slope of the curve when plotting ln $(1-(q/q^e))$ vs. time. If this rate of adsorption formula is valid, the values of K for each concentration should be the same. In the mixed-ion system, the average K value for the adsorption of Ca^{2+}

was found to be 0.0128 sec^{-1}. With known values of K and q^e defined by equation (4.1), this rate expression adsorption was then used to predict the exiting metal ion (e.g. Ca^{2+}) concentration in mixed-ion systems for adsorption in the following fixed bed operations.

4.3 Column Operation

4.3.1 Flow Characteristics of the Column in Fixed Bed Operation or No Adsorption Test

The simple kinetic model cannot be completed without knowing the flow characteristics in the system. Thus, the experiments in this part were carried out to determine the flow pattern in the column in fixed bed operation. The concept in this phase is to conduct experiments with no adsorption of metal ions so that the analytical solution of equation (2.18) can be used by treating the rate of adsorption equal zero. After being flushed with DI water to remove excess H^+ ions, the column was subject to the H^+ flow with H^+ ions acting as a tracer. The H^+ concentration was measured at the column exit by a pH probe. The comparison of hydrogen concentration between the experimental data and the predicted data of the no adsorption test is shown in Figure 4.7.

From Figure 4.7, it is apparent that the experimental data were fitted reasonably well with the mathematical model, which consists of one CSTR and one ideal PFR in series. From this exercise, the volume of the CSTR was determined to be 3.5 ml.

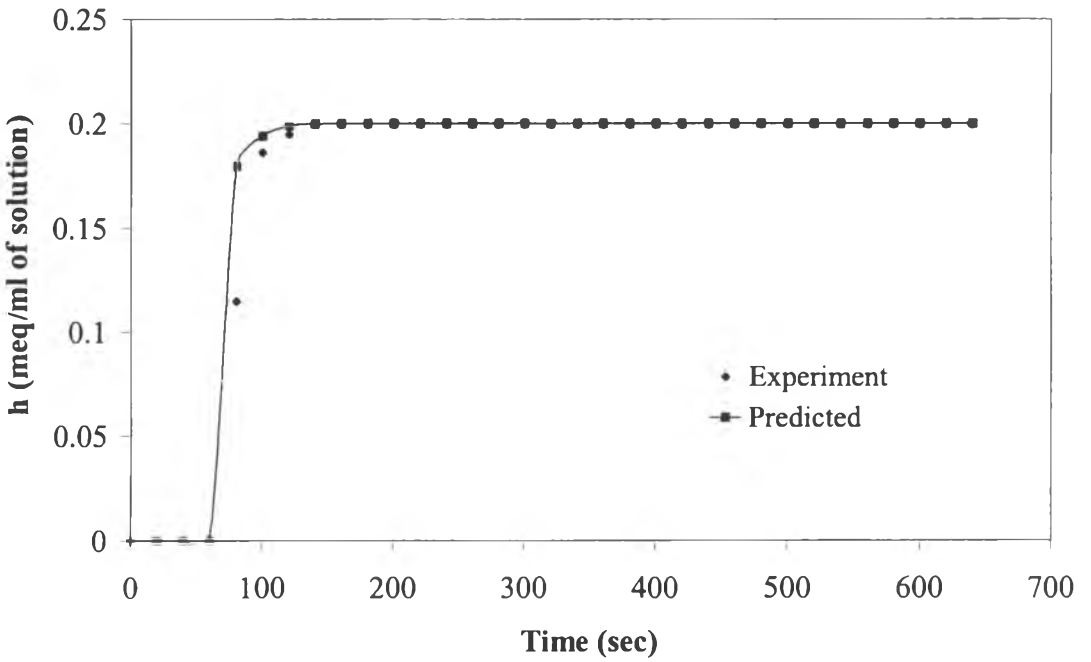

Figure 4.7 The comparison of the experimental data and the predicted data of the no adsorption test

4.3.2 Mathematical Modeling of Adsorption Kinetics of an Ion-Exchange Column in Fixed-Bed Operation

This part of the study concerns the application of the kinetic model described earlier to the multicomponent adsorption in downflow or fixed bed operation. The adsorption in the fixed-bed operation or downflow direction depends upon both distance along the column, x, and time, t, so the *method of characteristics for hyperbolic equations* was used to solve the problem. Fortunately, this method can be simplified by using the *conventional finite-difference* method presented by equations (2.18) and (2.19) instead. Equations (2.18) and (2.19), together with a completely *implicit approach*, were used to predict the concentration of Ca^{2+} ions in the mixed-ion solution, c, at any time t and distance along the column, x. A trigger cell was used to start the process by using the trigger cell and the logical function (how the trigger cell works and how it relates to the completely implicit method are described in Appendices E and C, respectively). The under-relaxation method was also used to protect the negative c value occurring in some step of iterations (how the under-relaxation works and how it relates to the completely implicit method are

described in Appendices F and C, respectively). The volume of the CSTR found from the no adsorption part and other kinetic parameters such as β, n and K, whose values found from batch operation were included in the mathematical model. In the adsorption model, the predicted exit value of hydrogen concentration, h, can be computed directly based on the concept: the solution must be electrically neutral. According to the fact that the hydrogen concentration in the solution at time t_i is equal the different value between initial calcium concentration and calcium concentration in the solution at time t_i. Figure 4.8 shows a comparison of the predicted and the experimental calcium concentrations in mixed-ion (Ca^{2+}/Mg^{2+}) solution measured at the exit of the ion exchange column with fixed bed operation.

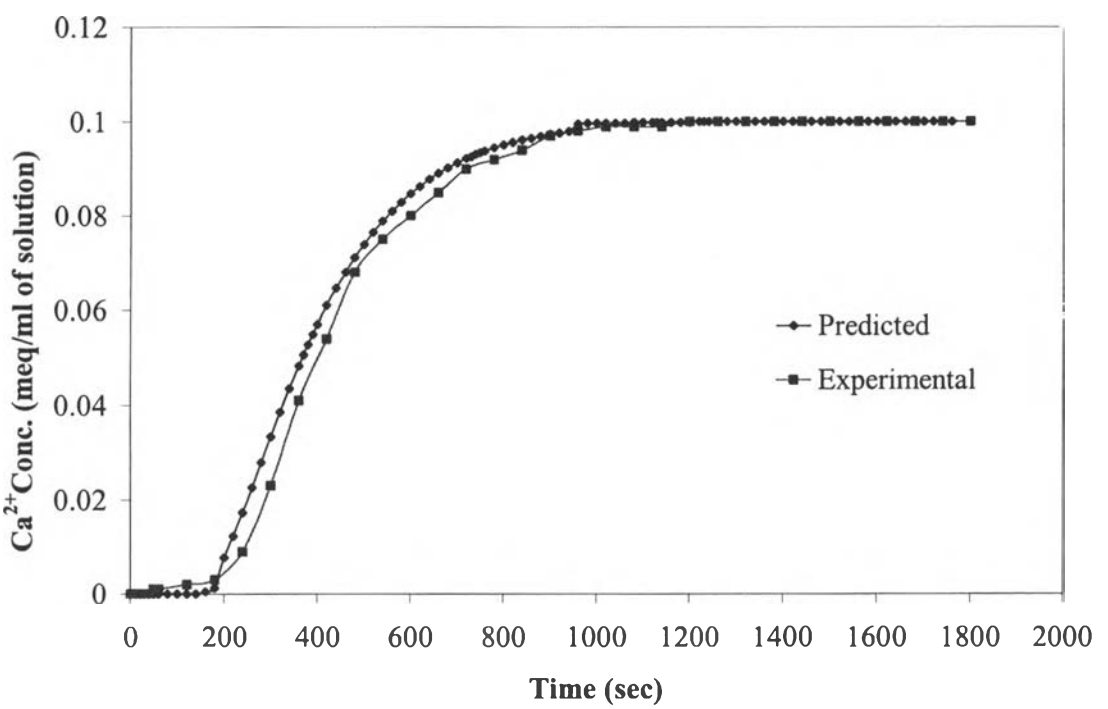

Figure 4.8 The comparison of the experimental data and the predicted data for calcium ions in mixed-ion system at the column exit with fixed-bed operation

From Figure 4.8, it can be seen that there is only small deviation between the predicted and experimental values, especially at the early phase of the adsorption course. In this phase, due to the high concentration gradient as discussed before the adsorption occurred very rapidly. Furthermore, the Ca^{2+} ions concentration profile in the experimental data is shift to the right hand side. In other

words, the Ca^{2+} ions exit from the column slower than those predicted from the model. Probably, the rate constant (K) in the model, which is obtained from analyzing the batch adsorption experiments, may be smaller than expected, giving the adsorption rate of the model smaller than the actual value. Consequently, this makes the predicted exit Ca^{2+} concentration coming out faster than the experimental value as seen in the breakthrough curve.

4.4 Analysis of Adsorption Kinetics of Single-Ion (Ca^{2+}, Mg^{2+}) and Mixed- Ion (Ca^{2+}/Mg^{2+}) Systems

Adsorption of metal ions (Ca^{2+} and Mg^{2+}) in both single-ion and mixed-ion systems were studied in order to investigate the competitive adsorption in both batch and fixed bed operations.

4.4.1 Batch Operation

From the single ion adsorption and the mixed-ion adsorption of Ca^{2+}, Mg^{2+} with equal ratio on Dowex50-x8 resin at initial metal concentrations of 0.2 N and 0.6 N (Figure 4.5 and 4.6), the initial adsorption rate can be calculated from the initial slope of the curve (see Appendix D) and the rates are shown in Table 4.4. In addition, the fractions of Ca^{2+} and Mg^{2+} ions adsorbed on Dowex50-x8 in mixed-ion system are shown in this table. The diagram of steps in determining the fraction of ion adsorbed onto the resins for batch operation is shown in Figure D1 (see Appendix D).

Table 4.4 Summary of initial rates and fractions of ions adsorbed onto the resins in batch systems

Type of system	Initial adsorption rate (meq/ml of resin*sec)		Fraction of ion adsorbed on to the resin (%)	
	Co= 0.2N	Co= 0.6N	Co= 0.2N	Co= 0.6N
Ca^{2+} in single-ion solution	0.0415	0.0527	-	-
Mg^{2+} in single-ion solution	0.0352	0.0436	-	-
Ca^{2+} in mixed-ion solution	0.0176	0.0352	61.17	65.13
Mg^{2+} in mixed-ion solution	0.0113	0.0295	38.83	34.87

From Table 4.4, the results show that the initial adsorption rates of Ca^{2+} ions both in single-ion and mixed-ion solutions are much higher than those of Mg^{2+} ions. It could be explained that the Dowex50-x8 resin has a preferential adsorption of Ca^{2+} ions over the Mg^{2+} ions. In this case, Ca^{2+} and Mg^{2+} ion have the equal valance electron, which is 2+, but the Ca^{2+} ions have the higher atomic number than the Mg^{2+} ions. According to this, it makes the size of Ca^{2+} ions smaller than Mg^{2+} ions, therefore, the Ca^{2+} ions are faster to adsorb and attached to the reactive sites on the Dowex50-x8 resin with the stronger bond.

In the mixed-ion system, the fractions of Ca^{2+} ions adsorbed onto the resin also are much higher than Mg^{2+} ions both in initial metal concentrations of 0.2 N and 0.6 N. The results mentioned above confirm the reason why the Dowex50-x8 has higher capability of adsorption for Ca^{2+} ions than Mg^{2+} ions.

Moreover, the comparisons between the adsorption of Ca^{2+} ions and Mg^{2+} ions onto the Dowex50-x8 resin in the single-ion and mixed-ion solutions for initial concentration 0.2 N are shown in Figure 4.9 and 4.10, respectively. It is obviously seen that the initial adsorption rates of both Ca^{2+} and Mg^{2+} ions in the single-ion system are higher than those in the mixed-ion solution, because there is no competitive ions present in the solution. There is only one type of ion adsorbed onto the resin resulting in high adsorption rate.

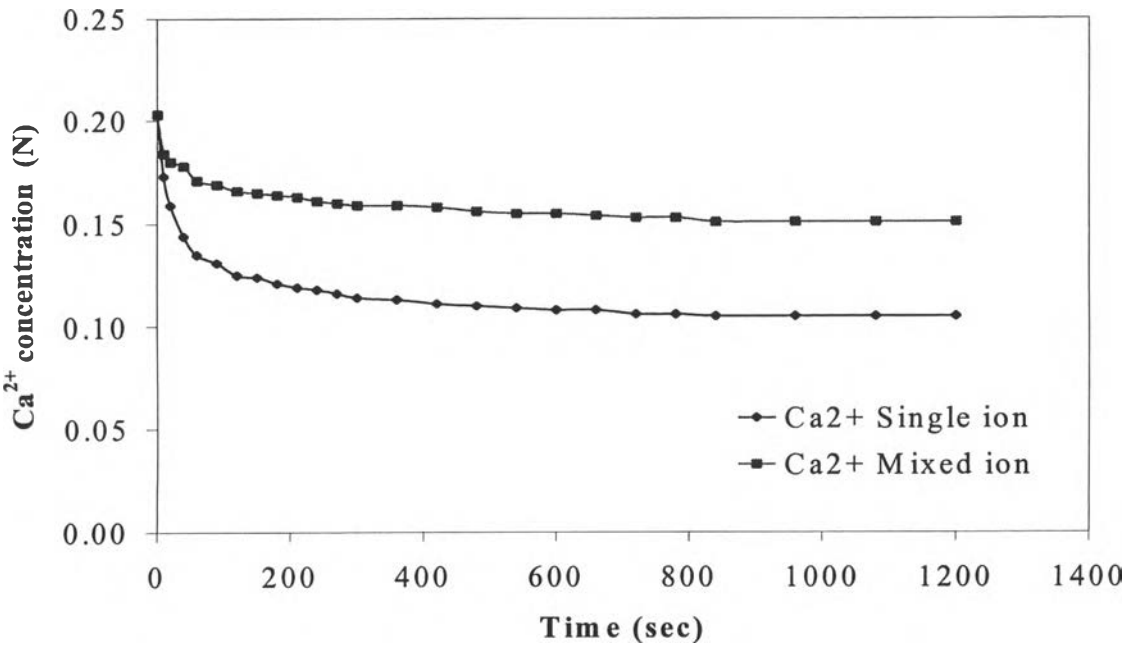

Figure 4.9 Comparison between the adsorption of Ca^{2+} ions onto Dowex50-x8 resin from the single-ion and mixed-ion solutions for C_0~ 0.2 N in batch operation

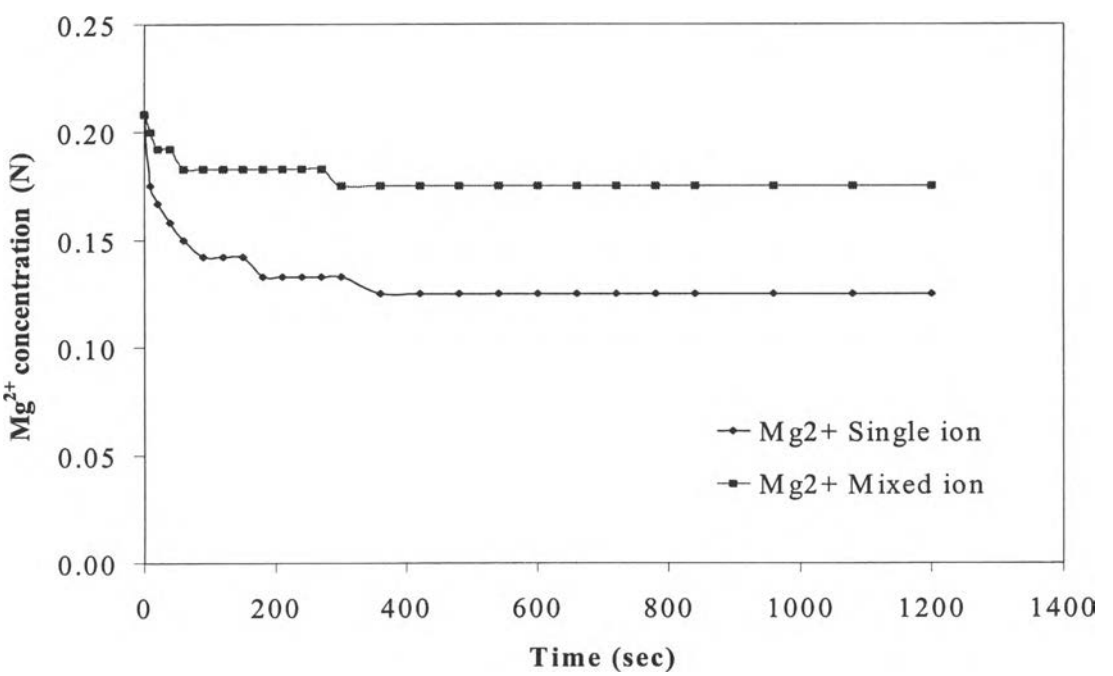

Figure 4.10 Comparison between the adsorption of Mg^{2+} ions onto Dowex50-x8 resin from the single-ion and mixed-ion solutions for C_0~ 0.2 N in batch operation

4.4.2 Fixed-Bed Operation

The objective in this phase is to study the effect of various initial metal concentrations on the adsorption and desorption (during regeneration) of metal ions from single-ion and mixed-ion solutions in fixed bed operation. The fraction of metal ions adsorbed onto the resin can be calculated from the ratio of adsorption capacity. On the other hand, the fraction of metal ions desorbed/regenerated from the resin can be determined from the desorption studies (involving regeneration by using 0.2 N HCl). From the adsorption and desorption results, the total number of ions adsorbed onto the resin (q_t), the maximum desorption rate (dc/dt), and the fraction of ion adsorbed onto the resin in various systems are shown in Table 4.5 and 4.6.

Table 4.5 Summary of the total number of ions adsorbed (q_t) and the fraction of ions adsorbed onto the resin for Ca^{2+}/Mg^{2+} ions in single-ion and mixed-ion solutions in fixed-bed operation

Type of system	q_t (meq/ml resin bed)		Fraction of ions adsorbed onto the resin (%)	
	C_0 = 0.1 N	C_0 = 0.2 N	C_0 = 0.1 N	C_0 = 0.2 N
Ca^{2+} in single-ion solution	2.170	2.965	-	-
Mg^{2+} in single-ion solution	1.506	-	-	-
Ca^{2+} in mixed-ion solution	1.279	2.656	58.06	61.24
Mg^{2+} in mixed-ion solution	0.745	1.228	41.94	38.76

Table 4.5 illustrates the adsorption of Ca^{2+} and Mg^{2+} ions onto the resin in both single-ion and mixed-ion systems at different initial metal concentrations. It is obvious that in the range of concentrations observed the amount of metal ions adsorbed onto the resin (q_t) is proportional to the initial metal concentration in both single-ion and mixed-ion systems. This relationship can be explained that a higher initial metal concentration results in increasing the driving force, which can overcome the mass transfer resistance in the solution and the resin

phases. Moreover, the higher initial metal concentration will have a beneficial effect on the saturation value of metal ion concentration adsorbed on the resin (q_t). In other word, the kinetics of the ion exchange have driven the system to a higher equilibrium point when increasing the initial metal concentration.

The total amount of both Ca^{2+} and Mg^{2+} ions adsorbed in the single-ion solution is higher than those in the mixed-ion solution (as shown in Table 4.5). The same reason as in the case of batch operation can be used to describe the results. In mixed-ion system, the fraction of metal ions adsorbed onto the resin represents equilibrium data or a thermodynamically limited process. The results indicate that the fraction of Ca^{2+} ions adsorbed onto the resin is higher than that of Mg^{2+} ions in fixed-bed operation, which is similar to the resulted observed in batch operation (Table 4.4). Again, the same reason can be offered as the selectivity value of Ca^{2+} ions on the Dowex50-x8 is higher than that of Mg^{2+} ions, so the resin prefers Ca^{2+} ions to Mg^{2+} ions.

Table 4.6 Summary of maximum desorption rate (dc/dt) and the fraction of metal ions regenerated both in single-ion and mixed-ion solution in fixed-bed operation

Type of system	Desorption rate (meq/ml resin*sec)		Fraction of ions regenerated (%)	
	$C_0 = 0.1$ N	$C_0 = 0.2$ N	$C_0 = 0.1$ N	$C_0 = 0.2$ N
Ca^{2+} in single-ion solution	0.00287	0.00165	52.92	43.42
Mg^{2+} in single-ion solution	0.00465	-	63.71	-
Ca^{2+} in mixed-ion solution	0.00280	0.00148	55.66	41.37
Mg^{2+} in mixed-ion solution	0.00386	0.00220	73.17	71.06

Note: The fraction of ions regenerated is defined as a ratio between the total number of ions desorbed from the resin (q_d) and adsorbed onto the resins (q_t).

During the regeneration, the desorption of Ca^{2+} and Mg^{2+} ions both in single-ion and mixed-ion solutions were studied by using 0.2 N HCl solution at flowrate 100 ml/min. The maximum desorption rate of Ca^{2+} and Mg^{2+} ions and the

fraction of ion regenerated in various systems can be calculated and are shown in Table 4.6. It can be seen that the maximum desorption rate of Mg^{2+} ions is much higher than that of Ca^{2+} ions for both single-ion and mixed-ion systems. In other words, Mg^{2+} ions were easily desorbed from the resin. This can be attributed to the low affinity of the Dowex50-x8 resin towards Mg^{2+} ions as compared to Ca^{2+} ions, so the Mg^{2+} ions were released from the resin faster than Ca^{2+} ions.

When the desorption is observed at different metal concentrations, the maximum desorption rates of Ca^{2+} and Mg^{2+} ions both in single-ion and mixed-ion system are inversely proportional to the initial metal concentration. The desorption rate of initial metal concentration of the 0.2 N is lower than that observed when the initial metal concentration of 0.1 N was used. The explanation is that the higher initial concentrations provide the higher capability of metal adsorbing onto the resin due to the higher driving force of concentration gradient. In other words, at high concentration, the metal ions can diffuse into the resin particle to the exchangeable sites, and may have the stronger attractive force than at lower initial concentration, thus, becoming difficult to desorb from the resin.

The fraction of metal ions regenerated (see calculations in Appendix D) when compared with the total number of metal ions adsorbed is shown in Table 4.6. It is demonstrated that in the mixed-ion systems, the fraction of Ca^{2+} and Mg^{2+} ions regenerated is higher than those in the single-ion systems. It can be explained that, with competitive ions being adsorbed onto the resin, the attraction force for adsorption is weaker when compared to the single-ion system, which has only one type of ions adsorbed onto the resin.